Supplementary Information

Pro-phagocytic function and structural basis of GPR84 signaling

Xuan Zhang [1, 2, &], Yujing Wang[1, &], Shreyas Supekar[3, &], Xu Cao[4], Laura Jenkins[5], Sara Marsango[5], Jingkai Zhou[4], Jessica Dang[4], Siqi Chen[4], Xiu Li[1], Guibing Liu[1], Graeme Milligan[5, *], Mingye Feng[4, *], Hao Fan[3, *], Weimin Gong[1, *], Cheng Zhang[2, *]

[1]Division of Life Sciences and Medicine, University of Science and Technology of China, Hefei, Anhui, China.

[2]Department of Pharmacology and Chemical Biology, University of Pittsburgh School of Medicine, University of Pittsburgh, Pittsburgh, PA 15261, USA.

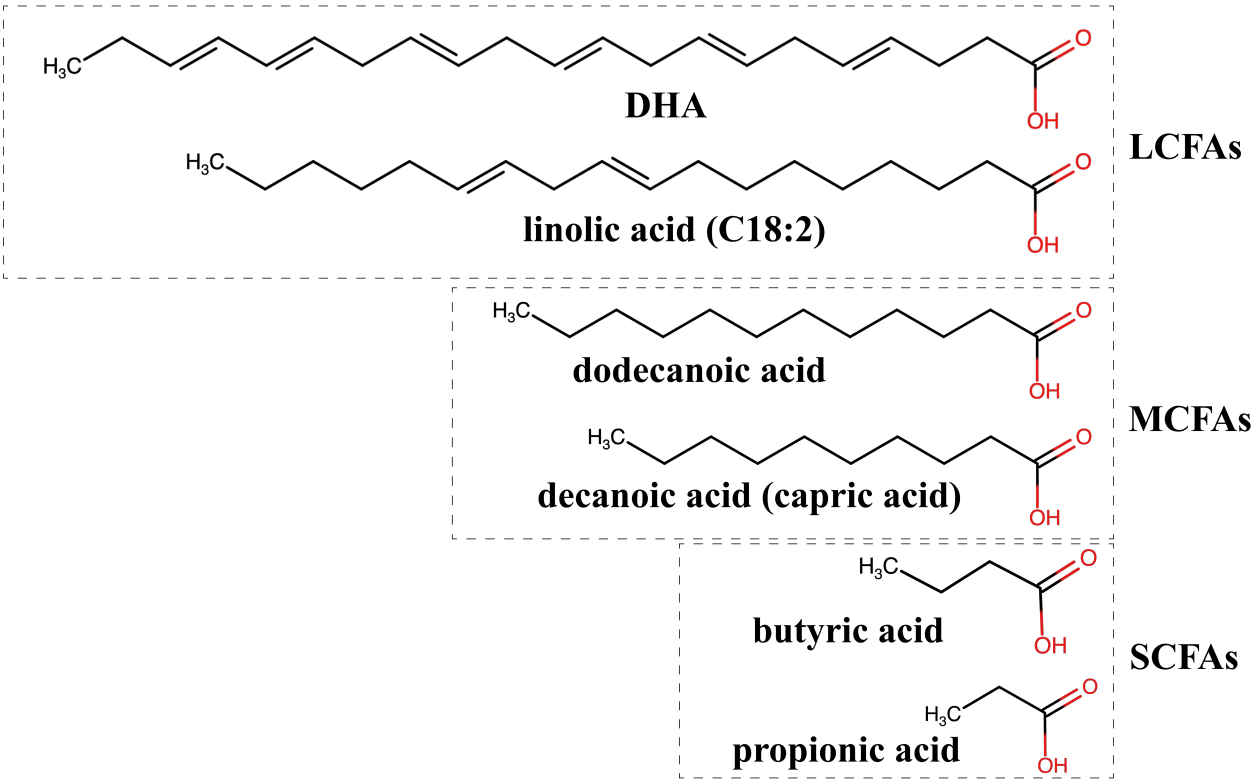
[3]Bioinformatics Institute (BII), Agency for Science, Technology and Research (A*STAR), 138671, Singapore.

[4]Department of Immuno-Oncology, Beckman Research Institute, City of Hope Comprehensive Cancer Center, Duarte, CA 91010, USA.

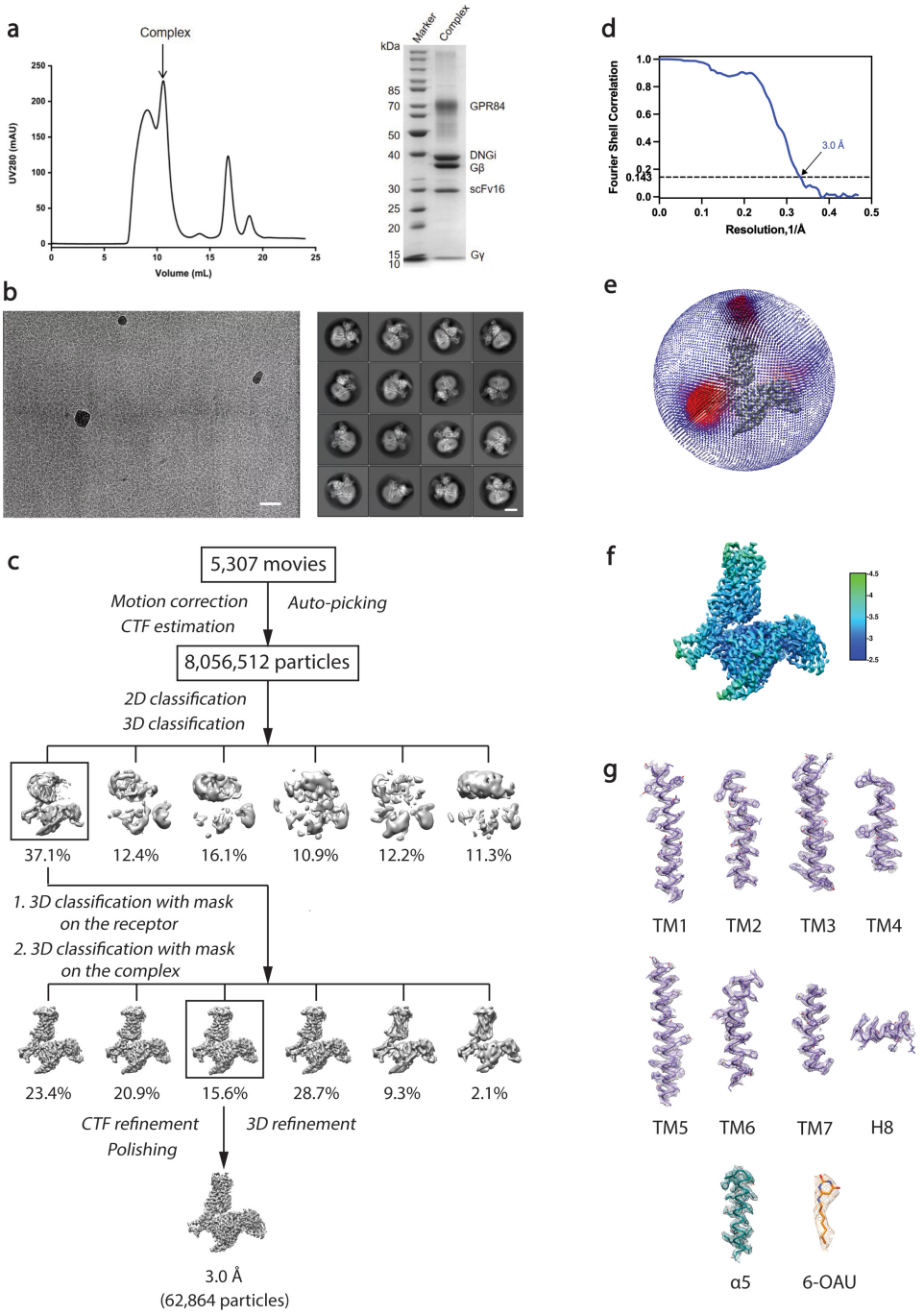
[5]Centre for Translational Pharmacology, School of Biomolecular Sciences, College of Medical, Veterinary and Life Sciences, University of Glasgow, Glasgow G12 8QQ, Scotland, U.K.

[&]Equal contribution

[*]Corresponding authors: G.M. (Graeme.Milligan@glasgow.ac.uk), M.F. (mfeng@coh.org), H.F. (fanh@bii.a-star.edu.sg), W.G. (wgong@ustc.edu.cn), C.Z. (chengzh@pitt.edu).

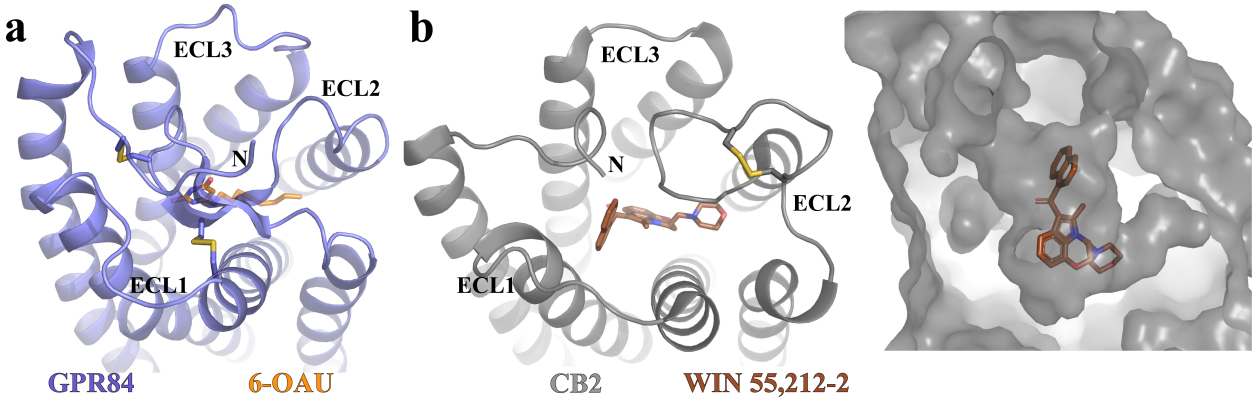


Supplementary Figure 1. Representative short-chain, medium-chain, and long-chain fatty acids (SCFAs, MCFAs, and LCFAs).

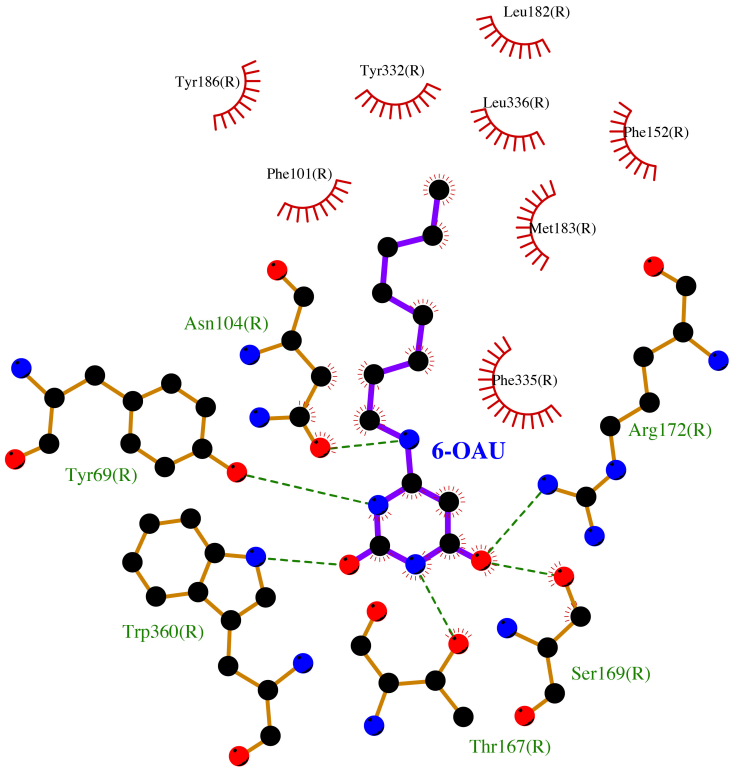


Supplementary Figure 2. Purification of the GPR84-G_i complex with 6-OAU and cryo-EM data processing. (a) Size-exclusion chromatography profile and SDS-PAGE analysis of the purified 6-OAU-GPR84-G_i complex. **(b)** Representative cryo-EM micrograph (scale bar: 50 nm) and 2D class averages (scale bar: 5 nm). **(c)** Cryo-EM image processing workflow for the 6-OAU-GPR84-G_i complex. **(d)** Gold-standard Fourier shell correlation (FSC) curve showing an overall resolution is 3.0 Å at FSC=0.143. **(e)** Angular distribution of the particles used in the final reconstruction. **(f)** Density map according to local resolution estimation. **(g)** Cryo-EM density

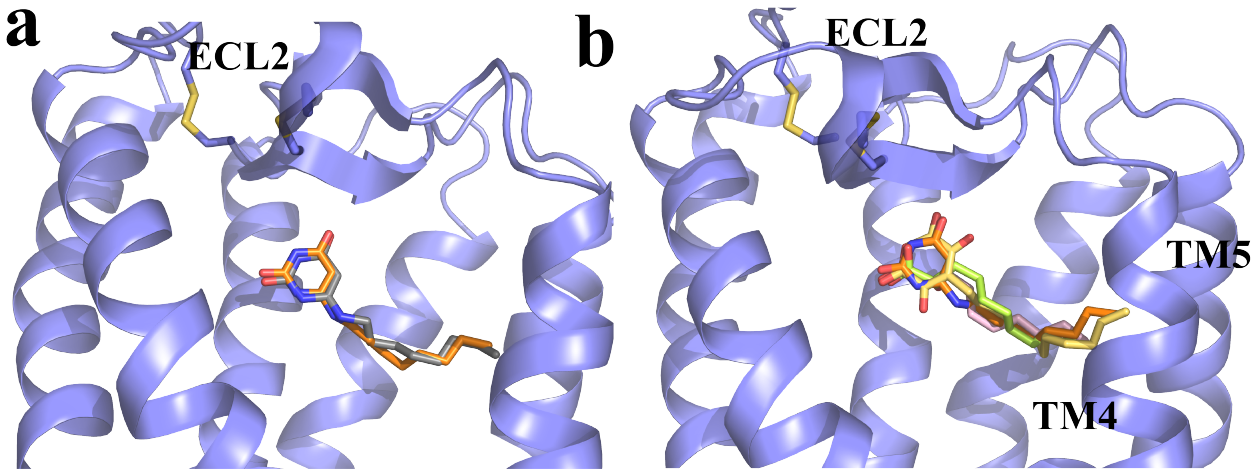
maps and models of the seven transmembrane helices (TM1-7), Helix 8 (H8), α5 helix of $G\alpha_i$ and the ligand of 6-OAU bound GPR84-Gi complex are shown. The EM density is shown at 0.0445 threshold.



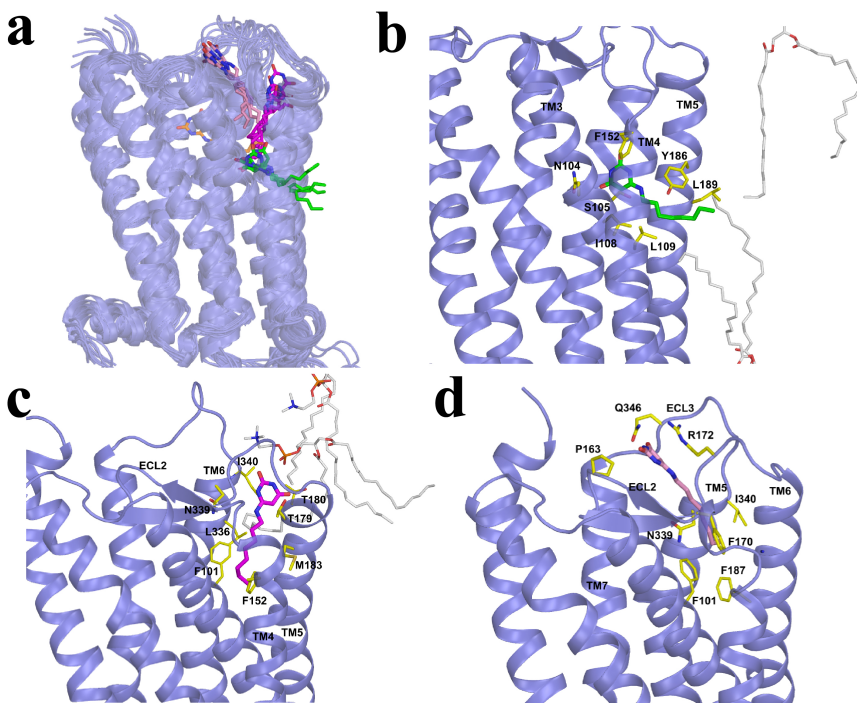
Supplementary Figure 3. Structural comparison with CB2. (a) Extracellular region of GPR84. **(b)** Extracellular region of CB2 and occluded ligand binding pocket. WIN 55,212-2 is a CB2 agonist. The figure is based on the CB2 structure with the PDB code 6PT0.



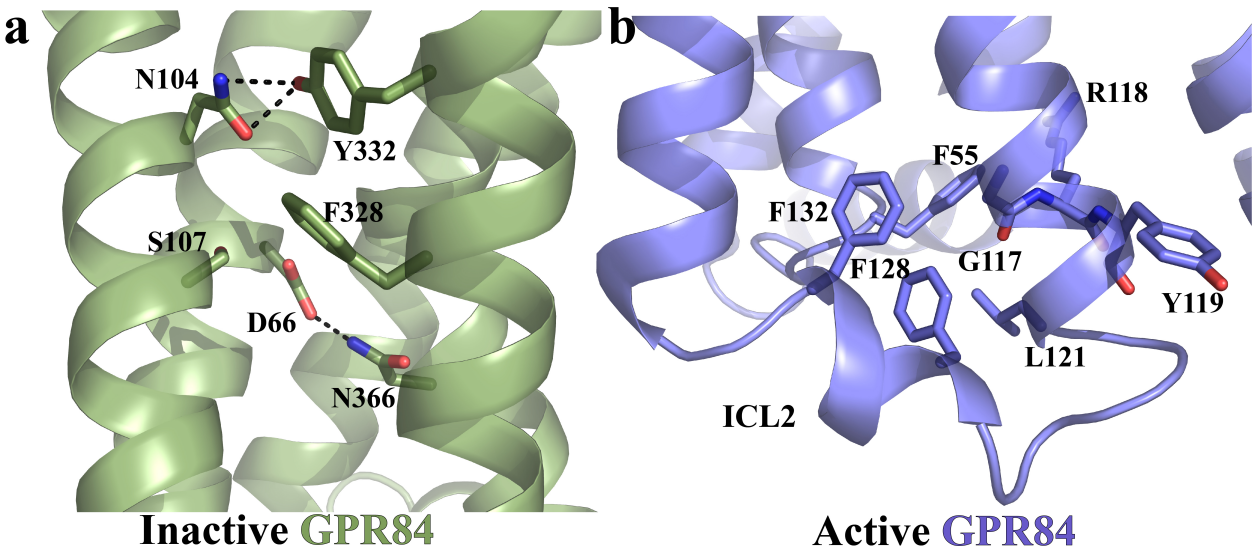
Supplementary Figure 4. Ligplot schematic representation of GPR84 interactions with 6-OAU. The carbon, nitrogen, and oxygen atoms are colored in black, blue, and red, respectively. Residues in GPR84 that form polar and hydrophobic interactions with 6-OAU are shown with green and black labels, respectively. Polar interactions are shown as green dashed lines. The ligand is shown as purple sticks.



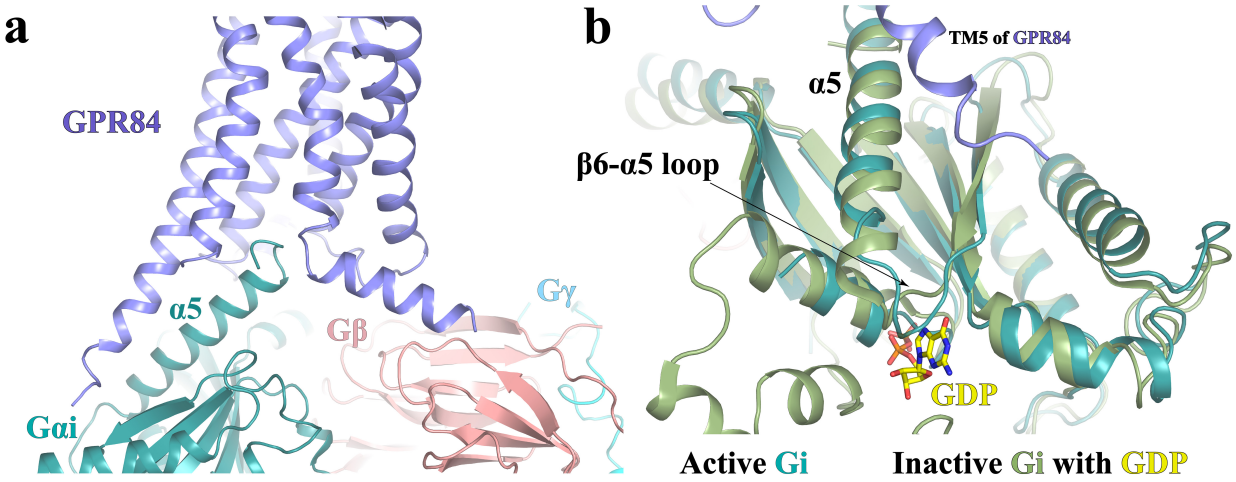
Extended Data Figure 5. Docking of GPR84 agonists. (a) Superimposition of docked 6-OAU (grey) and 6-OAU in our cryo-EM structure (orange). **(b)** Superimposition of docked embelin (light yellow), capric acid (pink), 2-hydroxyl capric acid (lime), and 6-OAU in our cryo-EM structure (orange).



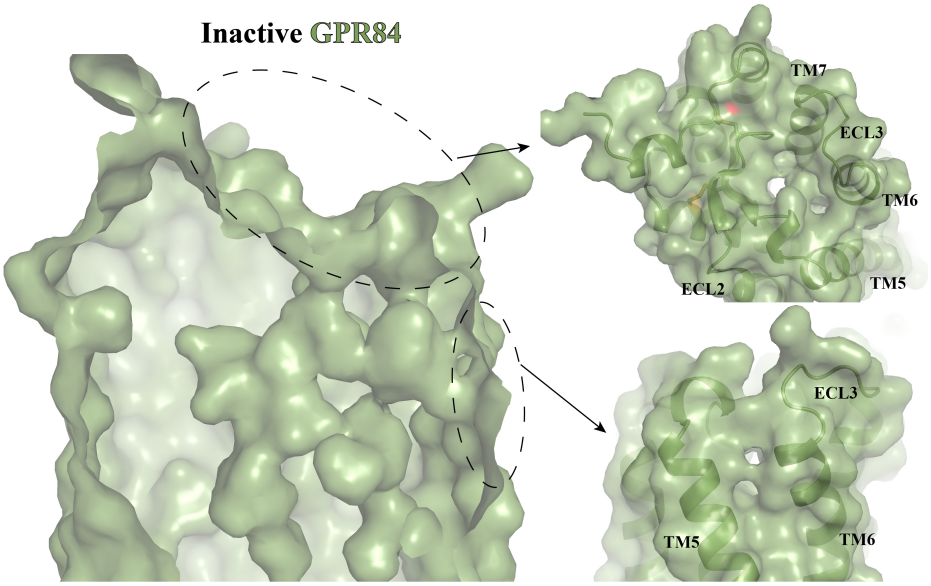
Extended Data Figure 6. Interactions of 6-OAU with GPR84 at three metastable sites. (a) Representative binding poses of 6-OAU at the metastable site S1 (green), S2 (magenta), and S3 (pink). 6-OAU in the cryo-EM structure is shown as orange sticks for reference. **(b)** S1 located at the interface between TM3-TM4-TM5 and membrane lipids where 6-OAU makes hydrophobic contacts with lipid tails and residues I108, L109, Y186, and L189. **(c)** S2 located at the interface between TM5-TM6 and membrane lipids where 6-OAU makes H-bonds with membrane lipid headgroups and hydrophobic contacts with F101, F152, M183, L336, and I340. **(d)** S3 located on top of the orthosteric site near the ECL2-ECL3-water interface where 6-OAU makes cation-π interaction with R172 (presumably acting as a gatekeeper residue) from ECL2, hydrogen bonds with Q346 from ECL3, and hydrophobic contacts with F101, F170, F187, and I340. Lipid molecules from the environment are shown as light grey sticks.



Extended Data Figure 7. (a) Residues at the core region of GPR84 in the Alphafold predicted inactive structure. **(b)** GRY motif and ICL2 in the active GPR84. Polar interactions are shown as dashed lines.



Extended Data Figure 8. Gi coupling and activation. (a) α5 of $G_{\alpha i}$ as the major interaction site for GPR84. GPR84 is colored in blue. Gαi, Gβ and Gγ subunits are colored in cyan, pink and light blue, respectively. **(b)** Conformational changes of α5 and the β6-α5 loop in Gαi during G protein activation and GDP release. The inactive Gαi with GDP is colored in light green. GDP is colored in yellow.



Extended Data Figure 9. Potential ligand binding pocket with openings in the Alphafold predicted inactive structure of GPR84.

Supplementary Table 1. Cryo-EM data collection and refinement statistics

	6-OAU-GPR84-Gi complex (EMD-29645, PDB 8G05)
Data collection and processing	
Magnification	81,000
Voltage (kV)	300
Electron exposure ($e^-/Å^2$)	55
Defocus range (μm)	-1.2 to -2.2
Pixel size (Å)	0.535
Symmetry imposed	C1
Initial particle images (no.)	8,056,512
Final particle images (no.)	62,864
Map resolution (Å)	3.0
FSC threshold	0.143
Map resolution range (Å)	2.5-4.5
Refinement	
Model resolution (Å)	3.1
FSC threshold	0.143
Model composition	
Non-hydrogen atoms	8955
Protein residues	1142
Ligand	1
Lipids	1
R.m.s. deviations	
Bond lengths (Å)	0.008
Bond angles (°)	0.923
Validation	
MolProbity score	1.45
Clashscore	4.43
Rotamer outliers (%)	0.72
Ramachandran plot	
Favored (%)	96.45
Allowed (%)	3.55
Disallowed (%)	0

Supplementary Table 2. Scores of docking 6-OAU, embelin, capric acid, and 2-hydroxy capric acid to the receptor cryo-EM structure.

Ligand	Docking score
6-OAU	-12.52
Embelin	-8.76
Capric acid	-4.45
2-hydroxy capric acid	-5.51